W-waveform Standing Surface Acoustic Waves with Two Equilibrium Positions under Linear Phase Modulation for Patterning Microparticles into Alternate Grid Patterns

Junseok Lee[1, a)]
School of Mechanical Engineering, Yonsei University, Seoul, Korea

(Dated: 11 November 2016)

This paper presents W-waveform Standing Surface Acoustic Waves (W-SSAW), and as its application, patterning of two groups of microparticles with different sizes alternately without fixing firstly patterned particles. W-SSAW is constructed by two standing surface acoustic waves of frequencies f and $2f$. Combined with linear phase modulation to translate Gor'kov potential at a constant speed, W-SSAW can selectively trap particles. The trapped particles follow the moving Gor'kov potential maintaining force equilibrium between Stokes' drag and the radiation force by W-SSAW. There exist two asymmetric equilibrium positions every period, and by the asymmetry, each group of particles is trapped at different equilibrium positions to form an alternate pattern. This technique is extended to two-dimensional alternate patterning by maintaining phase difference 90° between X- and Y-directional W-SSAWs. The patterning method utilizing W-SSAW is advantageous over SSAW-based patterning in that it does not require temporal separation to fix firstly patterned particles.

arXiv:1611.03446v1 [physics.flu-dyn] 10 Nov 2016

Recent scientific advances have enabled building substrates with desired patterns to accurately arrange micro- and nano-objects including living cells. Patterning cells and microparticles into desired arrangements is an important step in biological studies and applications such as tissue engineering, differentiation-on-a-chip, and cellar microenvironment manipulation.[1–3] In addition to passive methods that arrange micro-objects using prefabricated patterns, several active patterning methods that incorporate optics, electromagnetics, and acoustics have been demonstrated.[4–12] Especially, patterning with acoustic tweezers has been spotlighted due to the nature of acoustic waves which permits patterning of a mass of cells simultaneously without damaging or labeling cells.[13]

Surface acoustic wave (SAW) is an elastic wave traveling along the surface storing most of its energy within the surface. Two SAWs propagating in the opposite direction form standing SAW (SSAW), which exerts an acoustic radiation force on suspended particles as a result of scattering of the waves. The acoustic radiation force by SSAW moves particles with positive contrast factors to pressure nodes, and conversely, particles with negative ones to antinodes. Using SSAW, two-dimensional patterning of identical particles into the same pressure nodes is achieved.[12] In addition, patterning microparticles with positive contrast factors into pressure nodes, and particles with negative ones into antinodes to form alternate grid patterns is also accomplished.[14] However, when two groups of particles have the same sign of contrast factors, SSAW only arranges the particles at the same nodes or antinodes to form simple grid patterns [Fig. 1(a)]. Thus far, arranging particles with the same sign of contrast factor into an alternate grid pattern using SSAW has been based on temporal separation to fix the firstly patterned particles.[15] Only after one group of particles is firstly patterned and fixed on a substrate, the other group is patterned between them.

This paper presents a method of patterning particles alternately using W-waveform SSAW (W-SSAW). W-SSAW is constructed by two SSAWs that are of frequencies f and $2f$. It is shown that the radiation force exerted by W-SSAW on a particle equals linear addition of acoustic radiation forces by two SSAWs, and makes Gor'kov potential W-shaped to have asymmetry. On the other hand, when linear phase modulation is applied to W-SSAW to translate Gor'kov potential with a uniform speed, only particles that can maintain force equilibrium between Stokes' drag and the radiation force by W-SSAW are trapped by moving Gor'kov potential. From the asymmetry in Gor'kov potential, there emerge two asymmetric equilibrium positions, and each group of particles is trapped at different equilibrium positions forming an alternate grid pattern [Fig. 1(b)].

Two major forces in acoustofluidics are acoustic radiation force and Stokes' drag force. Acoustic radiation force is given as

$$\mathbf{F}_r = F_0 \sin(2kx)\,\hat{\mathbf{e}}_x, \tag{1a}$$

$$F_0 = \frac{\pi p_0^2 V_c \beta_w}{2\lambda}\varphi, \tag{1b}$$

where k, p_0, V_c, λ, and φ are wavenumber, acoustic pressure, the volume of the particle, wavelength, and contrast factor respectively.[16] The contrast factor is a material property, which is calculated as

$$\varphi = \frac{5\rho_c - 2\rho_w}{2\rho_c + \rho_w} - \frac{\beta_c}{\beta_w}, \tag{2}$$

where ρ_c, ρ_w, β_c and β_w are the density of the particle,

a)Electronic mail: junseok_lee@yonsei.ac.kr

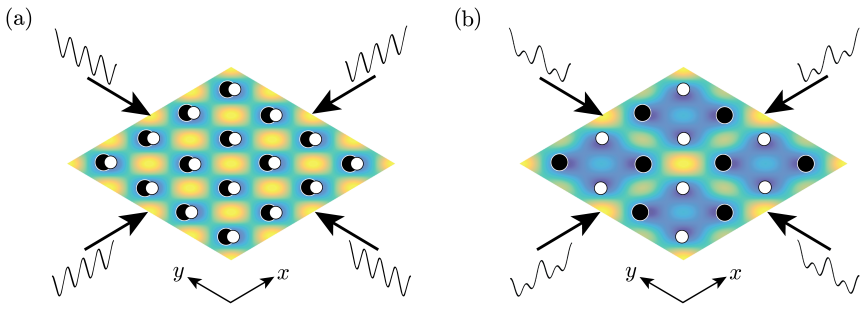

FIG. 1: **Comparison of patterning results using SSAW and W-SSAW, depicted on Gor'kov potentials.** Black and white spheres represent two groups of particles which have different sizes, but have the same sign of constrast factors. (a) Patterning utilizing SSAW cannot separate each group of particles into different positions, as Gor'kov potential of SSAW only has one equilibrium position every period. (b) In W-SSAW, there exist two asymmetric equilibrium positions every period. They allow each group of particles to be patterned into different equillibrium positions forming an alternate grid pattern.

the density of a fluid, the compressibility of the particle and the compressibility of the fluid. When phase modulation ϕ is applied, pressure nodes and antinodes are displaced by $\phi/2k$. Hence, acoustic radiation force can be obtained by substituting $x \to x-\phi/2k$ in Eq. (1a), giving

$$\mathbf{F}_r = F_0 \sin\left(2kx - \phi\right) \hat{\mathbf{e}}_x. \tag{3}$$

The Stokes' drag in a quiescent fluid is given as

$$\mathbf{F}_d = -b\mathbf{u}, \tag{4a}$$
$$b = 6\pi a\eta, \tag{4b}$$

where $\mathbf{u}$, and η are the particle velocity, and fluid viscosity, respectively.[17]

Acoustic radiation force is derived from $\mathbf{F}_r = -\nabla U$, where U is Gor'kov acoustic potential. The Gor'kov potential is given by

$$U = V_c \left[\xi_1 \frac{1}{2}\kappa_0 \left\langle p_{\text{in}}^2 \right\rangle - \xi_2 \frac{3}{4}\rho_0 \left\langle \mathbf{v}_{\text{in}}^2 \right\rangle\right], \tag{5}$$

where V_c, ρ_0, κ_0, p_{in}, $\mathbf{v}_{\text{in}}$, ξ_1 and ξ_2 are the volume of a particle, the density of a fluid, the compressibility of a fluid, the pressure field of incident wave, the velocity vector field of the wave, the monopole coefficient and the dipole coefficient, respectively.[18] The angle brackets represent time average operator.

Acoustic pressure field p_{ij} and velocity vector field $\mathbf{v}_{ij}$ of x_i-directional SSAW of frequency f_j are expressed as

$$p_{ij}\left(x_i, t\right) = A_{ij} \cos\left(k_{ij}x_i\right) \sin\left(\omega_{ij}t + \phi_{ij}\right), \tag{6a}$$
$$\mathbf{v}_{ij}\left(x_i, t\right) = v_{ij} \sin\left(k_{ij}x_i\right) \cos\left(\omega_{ij}t + \phi_{ij}\right) \hat{\mathbf{e}}_i, \tag{6b}$$

where A_{ij}, v_{ij}, k_{ij}, ω_{ij}, and ϕ_{ij} denote pressure amplitude, velocity amplitude, wave number, angular velocity and phase. From the superposition principle, the pressure fields and velocity fields of W-SSAW are obtained as

$$p_{1\text{w}} = p_{11}\left(x, t\right) + p_{12}\left(x, t\right), \tag{7a}$$
$$\mathbf{v}_{1\text{w}} = \mathbf{v}_{11}\left(x, t\right) + \mathbf{v}_{12}\left(x, t\right), \tag{7b}$$

where $p_{1\text{w}}$ and $\mathbf{v}_{1\text{w}}$ denote pressure field and velocity vector field of X-directional W-SSAW. The root mean square for $p_{1\text{w}}$ is expressed as

$$\begin{aligned}\left\langle p_{1\text{w}}^2 \right\rangle &= \left\langle A_{11}^2 \cos^2\left(k_{11}x\right) \sin^2\left(\omega_{11}t + \phi_{11}\right)\right\rangle + \left\langle A_{12}^2 \cos^2\left(k_{12}x\right) \sin^2\left(\omega_{12}t + \phi_{12}\right)\right\rangle \\ &\quad + \left\langle 2A_{11}A_{12} \cos\left(k_{11}x\right) \cos\left(k_{12}x\right) \sin\left(\omega_{11}t + \phi_{11}\right) \sin\left(\omega_{12}t + \phi_{12}\right)\right\rangle \\ &= \left\langle p_{11}^2 \right\rangle + \left\langle p_{12}^2 \right\rangle + 2A_{11}A_{12} \cos\left(k_{11}x\right) \cos\left(k_{12}x\right) \left\langle \sin\left(\omega_{11}t + \phi_{11}\right) \sin\left(\omega_{12}t + \phi_{12}\right)\right\rangle. \end{aligned} \tag{8}$$

Considering W-SSAW is comprised of two SSAWs of frequencies f and $2f$, from the orthogonality of trigonometric functions, the last term in Eq. (8) vanishes, giving

$$\left\langle p_{1\text{w}}^2 \right\rangle = \left\langle p_{11}^2 \right\rangle + \left\langle p_{12}^2 \right\rangle. \tag{9}$$

It should be noted that Eq. (9) holds true regardless of phase ϕ_{11} and ϕ_{12}. Similarly, the root mean square for $\mathbf{v}_{\text{in}}$ is expressed as

$$\left\langle \mathbf{v}_{1\text{w}}^2 \right\rangle = \left\langle \mathbf{v}_{11}^2 \right\rangle + \left\langle \mathbf{v}_{12}^2 \right\rangle. \tag{10}$$

By substituting Eqs. (9) and (10) into Eq. (5), we obtain

$$U_{1\text{w}} = U_{11} + U_{12}, \tag{11}$$

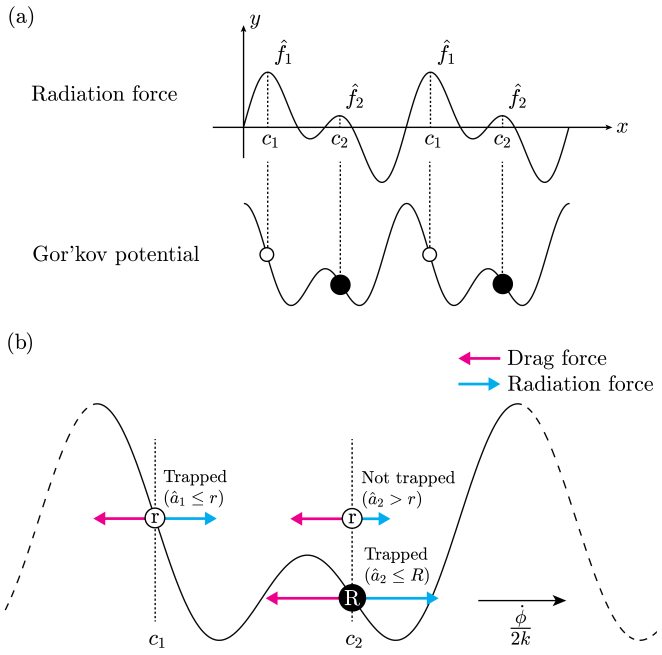

FIG. 2: (a) Acoustic radiation force of W-SSAW and two equilibrium positions in W-shaped Gor'kov potential under linear phase modulation. (b) The conditions for R-particles to be trapped at c_2, and r-particles at c_1. By lienar phase modulation, Gor'kov potential is moving at the speed of $\dot{\phi}/2k$. Trapped particles maintain force equilibrium between Stokes' drag and the radiation force.

where U_{11} and U_{12} are Gor'kov potentials of SSAWs of frequencies f and $2f$, respectively. Therefore, acoustic radiation force of W-SSAW is expressed as

$$\begin{aligned}\mathbf{F}_{1\mathrm{w}} &= -\nabla U_{1\mathrm{w}} = \mathbf{F}_{11} + \mathbf{F}_{12} \\ &= F_{01}\sin(2kx)\,\hat{\mathbf{e}}_x + F_{02}\sin(4kx)\,\hat{\mathbf{e}}_x,\end{aligned} \tag{12}$$

where $\mathbf{F}_{11}$ and $\mathbf{F}_{12}$ are acoustic radiation forces by SSAWs of frequencies f and $2f$, respectively. Therefore, the radiation force by W-SSAW can be estimated by adding acoustic radiation forces by two SSAWs when one frequency is twice the other frequency. To displace Gor'kov potential of W-SSAW by $\phi/2k$, phase modulations ϕ and 2ϕ are applied to two SSAWs of frequencies f and $2f$, respectively, since

$$\mathbf{F}_{1\mathrm{w}}\left(x-\frac{\phi}{2k}\right) = \mathbf{F}_{11}\left(x-\frac{\phi}{2k}\right) + \mathbf{F}_{12}\left(x-\frac{2\phi}{4k}\right). \tag{13}$$

For suspended particles subject to W-SSAW with phase modulation, the equation of motion is expressed by

$$b\frac{dx}{dt} = f\left(x-\frac{\phi}{2k}\right)V_c, \tag{14}$$

where $f(\cdot)$ denotes acoustic radiation force by W-SSAW per unit volume defined as $F_{1\mathrm{W}}(\cdot)/V_c$. Here, the inertia of a particle is neglected since viscous force dominates in microfluidics. It should be noted that as acoustic radiation force is proportional to the volume of a particle, $f(\cdot)$ is independent of V_c.

For fixed ϕ, a particle is attracted to minima of Gor'kov potential. When ϕ linearly increases, Gor'kov potential moves at a constant speed of $\dot{\phi}/2k$. Acoustic radiation force actuates the particle to follow the minima of moving Gor'kov potential, and the velocity of the particle is $\dot{\phi}/2k$. However, as the rate of phase modulation increases, the particle moves faster, and experiences larger drag force. When the increased drag force exceeds acoustic radiation force, the particle no longer follows the moving Gor'kov potential. Therefore, there exists the maximum rate of phase change for particles to be trapped, and it is obtained by equating the drag force and the maximum acoustic radiation force.

Suppose F_{11} and F_{12} in Eq. (12) are properly controlled for acoustic radiation force by W-SSAW per unit volume to have two local maxima $\hat{f}_1$ at c_1 and $\hat{f}_2$ at c_2, and $\hat{f}_1 > \hat{f}_2$ [Fig. 2(a)]. From the two local maxima, two maximum rates of phase change will be given. When drag force and the maximum acoustic radiation force are equal, Eq. (14) separates into

$$b\frac{dx}{dt} = \hat{f}_i V_c, \qquad x-\frac{\phi}{2k} = c_i, \tag{15}$$

where $i = 1, 2$. From Eq. (15), the phase to be modulated is given as

$$\phi = \frac{2k\hat{f}_i V_c}{b}t + 2kx_0 - 2kc_i, \tag{16}$$

where x_0 is the initial position of the particle. Hence, for spherical particles, the maximum rate of phase change $\dot{\Phi}$ for a particle of radius a to be trapped at equilibrium position c_i is

$$\dot{\Phi}_{i,a} = \frac{2k\hat{f}_i V_c}{b} = \frac{4k\hat{f}_i}{9\eta}a^2. \tag{17}$$

Rewriting Eq. (17) with respect to the radius gives

$$\hat{a}_i \le a, \qquad \hat{a}_i = \sqrt{\frac{9\eta}{4k\hat{f}_i}\dot{\phi}}, \tag{18}$$

where $\dot{\phi}$ denote the given rate of phase change, and $\hat{a}_i$ is defined to be the critical radius at c_i. It should be noted that from $\hat{f}_1 > \hat{f}_2$, $\hat{a}_1 < \hat{a}_2$.

As $\hat{a}_1 \neq \hat{a}_2$, the groups of particles to be trapped at c_1 and c_2 are different for a given rate of phase modulation. Suppose two groups of particles denoted by R-particles and r-particles are of radii R and r $(R > r)$, respectively. There exist two possible arrangements into which two groups of particles are separated and patterned:

(i) R-particles at c_2, and r-particles at c_1.
(ii) R-particles at c_1, and r-particles at c_2.

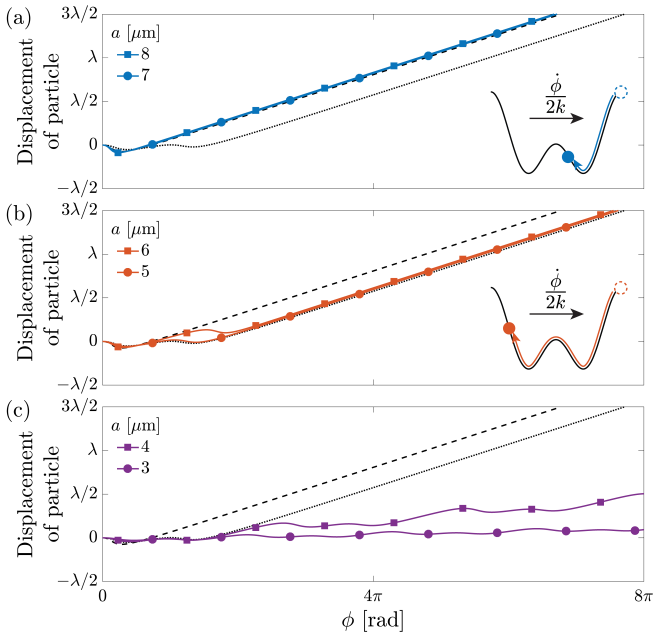

FIG. 3: **Displacements of particles with varius radii under linear phase modulation.** Dotted and dashed black lines represent displacements of particles of the critical radii $\hat{a}_1$ and $\hat{a}_2$, respectively. The *inset* shows the trajectories of particles to the trapped positions on Gor'kov potential. (a) Particles satisfying Eq. (19a) are trapped at c_2. (b) Particles satisfying Eq. (19b) are trapped at c_1. (c) The remaining particles are not captured by W-SSAW exhibiting oscillation.

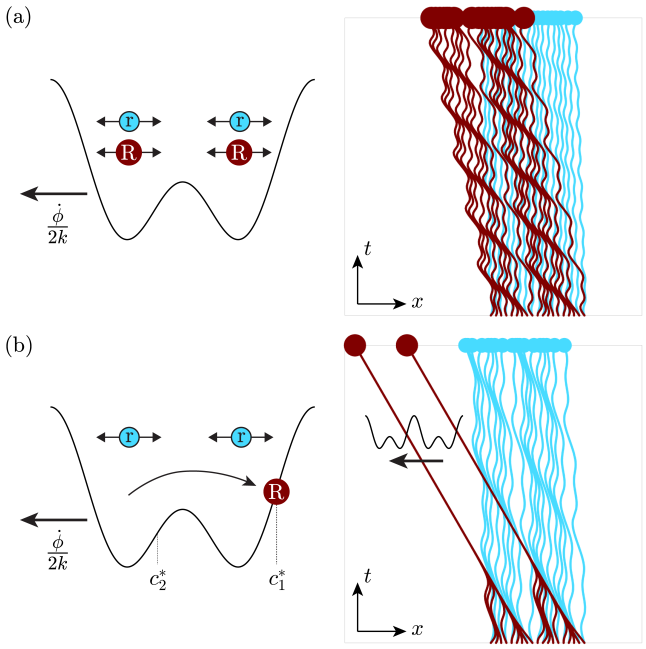

FIG. 4: **Motions and displacements of particles during the preprocess.** Red and blue spheres represent R- and r- particles, respectively. (a) The rate of phase change $\dot{\phi}$ is so high that both particles are not trapped by any equilibrium position but oscillate. (b) $\dot{\phi}$ is properly selected to trap and aggregate R-particles at c_1^*. The trajectories of r-particles remain dispersed due to oscillatory motion induced by high rate of phase change. c_1^* and c_2^* denote the corresponding positions of c_1 and c_2 when Gor'kov potential translates in the opposite direction, respectively.

Yet, the latter configuration is impossible. In the latter, r-particles are also trapped at c_1 as $\hat{a}_2 \leq r$ implies $\hat{a}_1 < r$. Moreover, R-particles can also be trapped at c_2 as $\hat{a}_2 \leq r$ satisfies $\hat{a}_2 < R$. Consequently, both R-particles and r-particles are able to be trapped in both equilibrium positions eliminating the asymmetry. Hence, we only consider the former arrangement, which requires the following conditions [Fig. 2(b)].

(i) R-particles must be trapped by the smaller maximum of the acoustic radiation force $\hat{f}_2$ to stay at c_2. From Eqs. (17) and (18),

$$\dot{\phi} \leq \dot{\Phi}_{2,R}, \qquad \hat{a}_2 \leq R. \tag{19a}$$

(ii) r-particles must be trapped by the larger maximum of the acoustic radiation force $\hat{f}_1$ to be trapped at c_1. From Eqs. (17) and (18),

$$\dot{\phi} \leq \dot{\Phi}_{1,r}, \qquad \hat{a}_1 \leq r. \tag{19b}$$

(iii) r-particles must not be trapped by the smaller maximum of the acoustic radiation force $\hat{f}_2$ to be passed to c_1. From the negation of Eqs. (17) and (18),

$$\dot{\phi} > \dot{\Phi}_{2,r}, \qquad \hat{a}_2 > r. \tag{19c}$$

Numerical analysis is performed with the material properties listed in Table S1 to show that two groups of particles are selectively trapped at each equilibrium position. The displacements of particles of various diameters are examined at the arbitrarily chosen rate of phase change. The result reveals that R-particles satisfying Eq. (19a) are trapped at c_2 [Fig. 3(a)], and r-particles satisfying Eq. (19b) at c_1 [Fig. 3(b)]. The remaining particles are not trapped by any equilibrium positions exhibiting oscillatory motion [Fig. 3(c)].

Since $\hat{a}_1 < R$, from Eq. (19b), R-particles are also able to be trapped at c_1. In other words, if R-particles are initially placed in the interval $I = [c_1, c_2)$, both R-particles and r-particles will be trapped at c_1. This problem can be tackled by the preprocess which positions R-particles in the outside of I. Though this preprocess can be achieved by conventional SSAW-based patterning methods, it is unfavorable in that SSAW aggregates not only R-particles but also r-particles into pressure nodes or antinodes. Once particles are aggregated, interparticle force arising from scattering of neighboring particles becomes dominant to invalidate Eq. (14).[19] In addition, the aggregation of particles has the effect of the aggregated particles having larger radius apparently. Considering W-SSAW separates particles depending on size difference, if r-particles aggregate

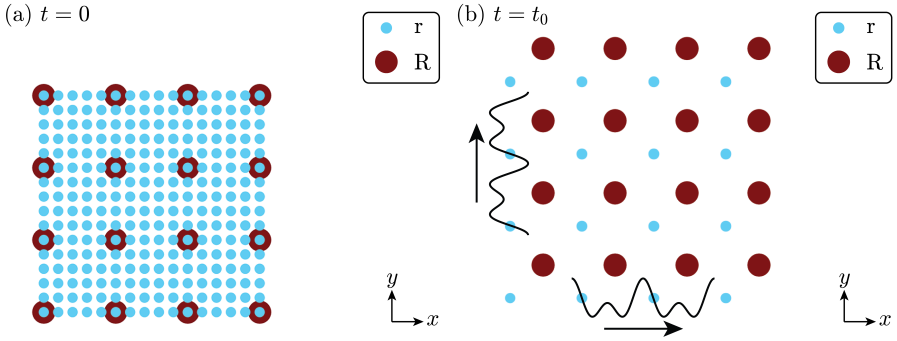

FIG. 5: **Results of the preprocess and two-dimensional alternate patterning.** (a) Initial arrangement of particles as a result of the preprocess using two-dimensional W-SSAW at the properly high rate of phase modulation. R-particles are patterned at c_1^*, whereas r-particles remain dispersed. (b) Two dimenional alternate patterning by X- and Y-directional W-SSAWs. R-particles are trapped at c_2, and r-particles at c_1 forming alternate grid patterns.

during the preprocess, separating out r-particles to c_1 becomes difficult. Hence, the preprocess should not aggregate r-particles.

Patterning R-particles without aggregating r-particles can be accomplished using W-SSAW at a properly high rate of phase modulation. When the rate of phase change is too high for both R- and r-particles to follow the moving Gor'kov potential, *i.e.*

$$\dot{\phi} > \max\left\{\dot{\Phi}_{1,R}, \dot{\Phi}_{1,r}, \dot{\Phi}_{2,R}, \dot{\Phi}_{2,r}\right\}, \tag{20}$$

both particles oscillates [Fig. 4(a)]. At gradually decreasing $\dot{\phi}$, one can find the rate of phase change satisfying

$$\dot{\Phi}_{1,R} \geq \dot{\phi} > \max\left\{\dot{\Phi}_{1,r}, \dot{\Phi}_{2,R}, \dot{\Phi}_{2,r}\right\}. \tag{21}$$

At that rate, only R-particles are trapped at c_1^*, the corresponding equilibrium position of c_1 in the opposite direction, which is in the outside of I [Fig. 4(b)]. It should be noted that r-particles stay dispersed. Hence, W-SSAW combined with the properly high rate of phase modulation can pattern R-particles without aggregation of r-particles.

One-dimensional W-SSAW can be extended to two-dimensional alternate patterning. Similar to Eq. (7), pressure field p_{in} and velocity vector field $\mathbf{v}_{\text{in}}$ of two-dimensional W-SSAW are superposed as

$$\begin{aligned} p_{\text{in}} &= p_{1\text{w}}(x,t) + p_{2\text{w}}(y,t) && \text{(22a)}\\ &= p_{11} + p_{12} + p_{21} + p_{22}, \\ \mathbf{v}_{\text{in}} &= \mathbf{v}_{1\text{w}}(x,t) + \mathbf{v}_{2\text{w}}(y,t) && \text{(22b)}\\ &= \mathbf{v}_{11} + \mathbf{v}_{12} + \mathbf{v}_{21} + \mathbf{v}_{22}, \end{aligned}$$

where $p_{2\text{w}}$ and $\mathbf{v}_{2\text{w}}$ are pressure field and velocity vector field of Y-directional W-SSAW. The root mean square for p_{in} is expressed as

$$\langle p_{\text{in}}^2\rangle = \langle p_{11}^2\rangle + \langle p_{12}^2\rangle + \langle p_{21}^2\rangle + \langle p_{22}^2\rangle + 2\Big(\langle p_{11}p_{12}\rangle + \langle p_{21}p_{22}\rangle + \langle p_{11}p_{22}\rangle + \langle p_{12}p_{21}\rangle\Big) + 2\Big(\langle p_{11}p_{21}\rangle + \langle p_{12}p_{22}\rangle\Big) \tag{23}$$

$$= \langle p_{11}^2\rangle + \langle p_{12}^2\rangle + \langle p_{21}^2\rangle + \langle p_{22}^2\rangle + 2\Big(\langle p_{11}p_{21}\rangle + \langle p_{12}p_{22}\rangle\Big). \tag{24}$$

The terms in the first parenthesis in Eq. (23) vanishes due to the orthogonality of trigonometric functions as in Eq. (8). On the other hand,

$$\begin{aligned} \langle p_{11}p_{21}\rangle &= A_{11}A_{21}\cos(kx)\cos(ky)\langle\sin(\omega t + \phi_{11})\sin(\omega t + \phi_{21})\rangle \\ &= A_{11}A_{21}\cos(kx)\cos(ky)\cdot\frac{1}{2}\cos(\phi_{11} - \phi_{21}). \end{aligned} \tag{25}$$

When $\phi_{11} - \phi_{21} = \pm\pi/2$, Eq. (25) vanishes. Similarly, choosing $\phi_{12} - \phi_{22} = \pm\pi/2$, we have $\langle p_{12}p_{22}\rangle = 0$. Hence,

$$\langle p_{\text{in}}^2\rangle = \langle p_{1\text{w}}^2\rangle + \langle p_{2\text{w}}^2\rangle. \tag{26}$$

On the other hand, using $\langle \mathbf{v}_{11}\cdot\mathbf{v}_{21}\rangle = \langle \mathbf{v}_{12}\cdot\mathbf{v}_{22}\rangle = 0$,

$$\langle \mathbf{v}_{\text{in}}^2\rangle = \langle \mathbf{v}_{1\text{w}}^2\rangle + \langle \mathbf{v}_{2\text{w}}^2\rangle. \tag{27}$$

From Eq. (5), Gor'kov potential of two-dimensional W-SSAW denoted by $U(x,y)$ is expressed as

$$U(x,y) = U_{1\text{w}}(x) + U_{2\text{w}}(y), \tag{28}$$

where $U_{2\text{w}}$ denotes Gor'kov potential of Y-directional W-SSAW. Therefore, acoustic radiation force for two-dimensional W-SSAW denoted by $\mathbf{F}(x,y)$ is given by

$$\mathbf{F}(x,y) = \mathbf{F}_{1\text{w}}(x) + \mathbf{F}_{2\text{w}}(y), \tag{29}$$

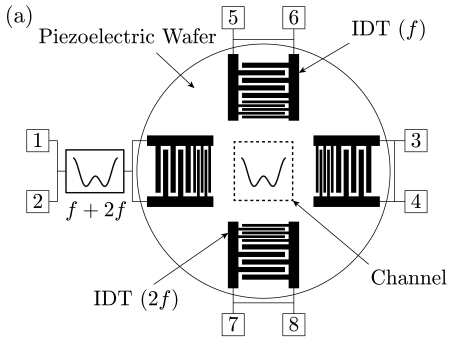

(b)

Port	Frequency	Phase
1	$f + \Delta f/2$	$\phi_{11}/2$
2	$2f + 2\Delta f/2$	$\phi_{12}/2$
3	$f - \Delta f/2$	$\phi_{11}/2$
4	$2f - 2\Delta f/2$	$\phi_{12}/2$
5	$f + \Delta f/2$	$\phi_{21}/2$
6	$2f + 2\Delta f/2$	$\phi_{22}/2$
7	$f - \Delta f/2$	$\phi_{21}/2$
8	$2f - 2\Delta f/2$	$\phi_{22}/2$

FIG. 6: (a) Experimental setup for two-dimensional alternate patterning using W-SSAW. (b) Configuration of frequency and phase of each port of a function generator. The shifted freqeuencies are to simulate linear phase modulation. The phase differences between X- and Y-directional W-SSAWs are maintained as 90°.

where $\mathbf{F}_{2\mathrm{w}}$ is acoustic radiation force for Y-directional W-SSAW. As Eqs. (4a) and (29) can be decoupled into X- and Y-directional components, the equation of motion is decoupled. It is followed that two-dimensional alternate patterning is performed by applying one-dimensional alternate patterning independently in each direction.

Numerical analysis using Particle Tracing Module in COMSOL Multiphysics® is performed to show two-dimensional alternate patterning. Suppose the preprocess has already been performed, so that R-particles are initially placed at c_1^*, and r-particles are randomly distributed [Fig. 5(a)]. The result shows that two-dimensional W-SSAW is capable of patterning particles alternately in two-dimension to create an alternate grid pattern [Fig. 5(b)].

In the experiment, two pairs of interdigital transducers (IDT) is prepared to radiate two SSAWs of frequencies f and $2f$ to generate W-SSAW [Fig. 6(a)]. As the bandwidth of an IDT is narrow enough that a pair of IDTs designed for a certain frequency only generates SSAW of the designed frequency. It implies that even if the combined signal of two frequencies is applied, each IDT only radiates its corresponding frequency from the mixed signal. Linear phase modulation can be simulated by shifting frequency. For example, on port 1,

$$\begin{aligned} y &= y_0 \cos(kx - 2\pi f t + (\dot{\phi}/2)t + \phi_{11}/2) \\ &= y_0 \cos\left(kx - 2\pi\left(f + \Delta f/2\right)t + \phi_{11}/2\right), \end{aligned} \tag{30}$$

where $\Delta f = \dot{\phi}/2\pi$. Similarly, the frequency and the phase of each port can be determined to have phase differences between X- and Y-directional W-SSAW and to simulate linear phase modulation [Fig. 6(b)]. Again, $\phi_{11} - \phi_{21} = \pm\pi/2$ and $\phi_{12} - \phi_{22} = \pm\pi/2$ must be maintained.

The acoustic method of patterning microparticles into an alternate grid pattern using W-SSAW is developed. From the orthogonality of trigonometric function, W-SSAW constructed by two SSAWs of f and $2f$ is shown to have W-shaped Gor'kov potential. When linear phase modulation is applied to W-SSAW, there emerge two asymmetric equilibrium positions for particles to be trapped. By the asymmetry, R- and r-particles are positioned into different equilibrium positions to have an alternate pattern. Furthermore, two-dimensional patterning is achieved by controlling the phase differences 90° in X- and Y-directional W-SSAWs. Moreover, the potential strength is that W-SSAW can pattern three or more than groups of particles into alternate grid patterns simultaneously. Specifically, when three SSAWs of frequencies f, $2f$, and $3f$ are superposed, similar to two SSAWs, acoustic radiation force by three SSAWs can be estimated by linear addition. One can, then, find three different local maxima to have three asymmetric conditions for particles to be trapped. Hence, three or more than groups of particles can be patterned to form complex grid pattern. It is believed that patterning different groups of particles into an alternate grid pattern using W-SSAW is beneficial for biological applications such as tissue engineering.

[1] M. M. Stevens, M. Mayer, D. G. Anderson, D. B. Weibel, G. M. Whitesides, and R. Langer, Biomaterials **26**, 7636–7641 (2005).
[2] A. Tourovskaia, X. Figueroa-Masot, and A. Folch, Lab on a Chip **5**, 14–19 (2005).
[3] C. A. Goubko and X. Cao, Materials Science and Engineering: C **29**, 1855–1868 (2009).
[4] D. G. Grier, Nature **424**, 810–816 (2003).
[5] K. Ino, M. Okochi, N. Konishi, M. Nakatochi, R. Imai, M. Shikida, A. Ito, and H. Honda, Lab on a Chip **8**, 134–142 (2008).
[6] H. Lee, A. Purdon, and R. Westervelt, Applied physics letters **85**, 1063 (2004).
[7] H. Lee, Y. Liu, D. Ham, and R. M. Westervelt, Lab on a Chip **7**, 331–337 (2007).
[8] D. R. Albrecht, G. H. Underhill, T. B. Wassermann, R. L. Sah, and S. N. Bhatia, Nature methods **3**, 369–375 (2006).
[9] D. S. Gray, J. L. Tan, J. Voldman, and C. S. Chen, Biosensors and Bioelectronics **19**, 771–780 (2004).
[10] N. Mittal, A. Rosenthal, and J. Voldman, Lab on a Chip **7**, 1146–1153 (2007).
[11] A. Rosenthal and J. Voldman, Biophysical Journal **88**, 2193–2205 (2005).
[12] J. Shi, D. Ahmed, X. Mao, S.-C. S. Lin, A. Lawit, and T. J. Huang, Lab on a Chip **9**, 2890–2895 (2009).
[13] X. Ding, P. Li, S.-C. S. Lin, Z. S. Stratton, N. Nama, F. Guo, D. Slotcavage, X. Mao, J. Shi, F. Costanzo, et al., Lab on a Chip **13**, 3626–3649 (2013).
[14] C. E. Owens, C. W. Shields, D. F. Cruz, P. Charbonneau, and G. P. López, Soft matter **12**, 717–728 (2016).
[15] F. Gesellchen, A. Bernassau, T. Dejardin, D. Cumming, and M. Riehle, Lab on a Chip **14**, 2266–2275 (2014).
[16] D. J. Collins, B. Morahan, J. Garcia-Bustos, C. Doerig, M. Plebanski, and A. Neild, Nature communications **6** (2015).
[17] H. Bruus, Lab Chip **11**, 3742 (2011).
[18] H. Bruus, Lab Chip **12**, 1014 (2012).
[19] T. Laurell, F. Petersson, and A. Nilsson, Chemical Society Reviews **36**, 492–506 (2007).

SUPPLEMENTARY MATERIAL

Material Properties			
Water			
Viscosity	η	0.98	mPa s
Compressibility	β_w	448	1/TPa
Density	ρ_w	998	kg/m^3
Polystyrene Particles			
Compressibility	β_c	249	1/TPa
Density	ρ_c	1050	kg/m^3
Diameter of R-Particle	$2R$	15	µm
Diameter of r-Particle	$2r$	10	µm
Acoustic Waves			
Acoustic Pressure	p_0	100	kPa
Wavelength	λ	280	µm
W-SSAW			
Rate of Phase Change	$\dot{\phi}$	8	rad/s
First Critical Radius†	$\hat{a}_1$	9.20	µm
Second Critical Raidus†	$\hat{a}_2$	13.2	µm

† Calculated from Eq. (18)

TABLE S1: Properties used for the numerical analysis.